Materials Research Proceedings 41 (2024) 271-282 https://doi.org/10.21741/9781644903131-31

Machine learning application for optimization of laser directed energy deposition process for aerospace component rapid prototyping in additive manufacturing

ERTUGRUL Gökhan[1,a *], ALIMOV Artem[1,b], SVIRIDOV Alexander[1,c] and HÄRTEL Sebastian[1,d]

[1]Chair of Hybrid Manufacturing, Brandenburg University of Technology, Cottbus, Germany

[a]Gökhan.Ertugrul@b-tu.de, [b]alimov@b-tu.de, [c]sviridov@b-tu.de, [d]Sebastian.Haertel@b-tu.de

Keywords: Directed Energy Deposition, Additive Manufacturing, Machine Learning, Digital Twin, Rapid Prototyping

Abstract. The paper proposes a methodology for determining the optimal L-DED parameters based on the minimum number planned of L-DED trials. A dataset compiled from planned L-DED experiments was used to train a machine learning model. The algorithm demonstrated a robust ability to predict the output metrics with notable accuracy and proposed a theoretical framework that modeled the complex relationships between the input variables and the resulting critical welding properties for AM. The application of the developed model and its comparison with conventional methods thus offers a methodical approach to determining the optimum process parameters in advance. This is a step towards the development and production of additively manufactured components for future digital twin application in the aerospace industry.

Introduction

The sustained development of additive manufacturing (AM) technologies such as laser directed energy deposition (L-DED) has evolved significantly, promoting extensive research into the improvement of processes and materials. Production of functionally graded materials, tool industry, repair and maintenance, medical implants, and production of aerospace parts are some of the applications of the L-DED process [1]. To achieve a deposition, a laser heat source has to provide sufficient energy to melt the substrate and the powder simultaneously in this process. Traditionally, the width, height, and penetration depth of weld beads have been used as essential metrics to evaluate the overall strength and quality of 3D parts made using AM [2]. The laser power, travel speed, powder feed rate, hatch distance, z-axis distance, and combination of these parameters are crucial to identify the geometry of the deposition with sufficient heat input (HI) in AM with L-DED. Considering these parameters and their combinations, the high precision and complexity of the L-DED process require highly efficient and accurate use of optimization techniques to achieve identified deposition such as artificial neural network (ANN) and machine learning (ML) methods. However, small datasets often make it difficult for learning algorithms to achieve accurate predictions, and an oversampling technique is needed to overcome this problem in ANN and ML [3]. ML provides higher accurate results than ANN for a limited training dataset [4]. New methodologies are required to decrease experimental costs and the number of datasets to store and process it. Therefore, the effectiveness of the experimental design to generate high quality datasets is important. Central composite design (CDD) and response surface methodology (RSM) are often used to design the experiment matrix in the weld process involving the lowest possible number of experiments [2]. Yi et al [4] discussed the use of ML with small datasets for wear prediction in AM. Zhu et al [5] applied ML with a small dataset for the inspection of surface morphology in DED. Xiong et al [6] used ANN with a small dataset to predict the bead geometry of GMAW.

Although there are some reports on DED concerning process dynamics, materials, and test planning, only a few of them focus on process or quality optimization involving a small dataset ML approach from the initial to the final product [2]. In this study, process parameter optimization is performed and compared using a small dataset applying statistical methods, ML, and a hybrid approach, which is a combination of these methods. Additive manufacturing was carried out with the optimized data and the final product was manufactured for the aerospace industry.

Material and Methods

The used material was spherical powder made of 316L (1.4404) with a grain size of 45 - 90 µm. The substrate plate made of the austenitic CrNi material 1.4301 had the dimensions 100 X 100 X 10 mm and was free of oxide layers.

A LUNOVU e-LMD system was used for the L-DED process. The L-DED system consisted of a 2.5 kW solid-state laser source, a coaxial nozzle with corresponding powder feed, 5-axis kinematics and a line scanner (Figure 1). The laser wavelength and spot diameter were 960 – 1080 nm and 1.6 mm respectively. Argon (99.998%) with a volume flow of 12 l/min was used as the shielding gas. The volume flow of the powder carrier gas was 3 l/min. The distance between the substrate and the nozzle was 13 mm in order to focus the laser and the powder on the molten pool. Rhino and LunoCAM slicer were used for computer aided design (CAD) and computer aided manufacture (CAM).

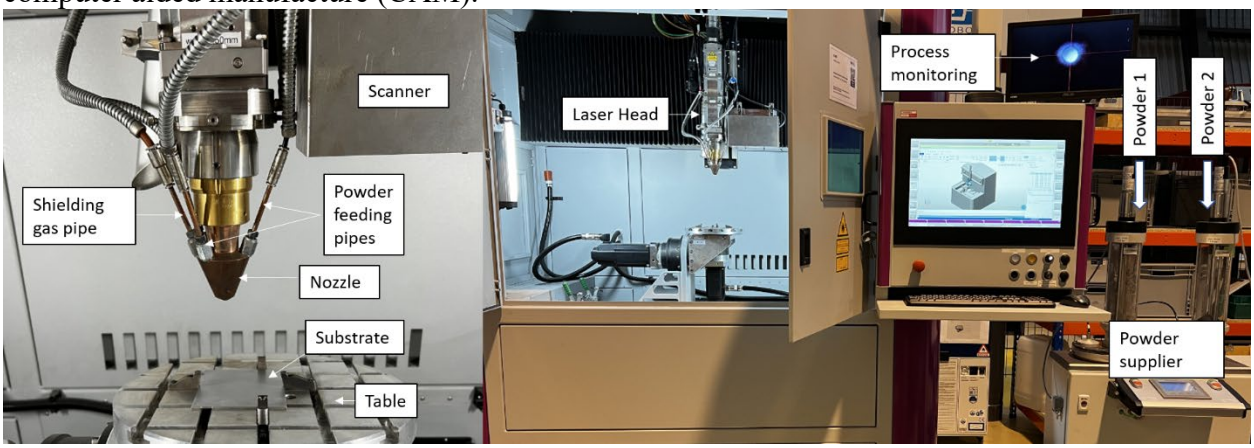

Figure 1. Labelled photograph of the L-DED system which was used to produce the samples characterises in this work.

Figure 2 shows the steps involved in optimizing the welding parameters for AM. The laser power, travel speed, and powder flow rate of 1.4404 material were investigated for a single layer related to weld width, weld height, aspect ratio (Weld width/Weld height), and dilution (100 * Penetration Area / (Penetration Area + Weld Bead Area)). The penetration area is the weld deposition area below the surface of the substrate and the weld bead area is the deposition area above the surface of the substrate. Subsequently, the optimized single weld parameters were adapted first coating with different hatch distances and AM with optimization of z-axis distance.

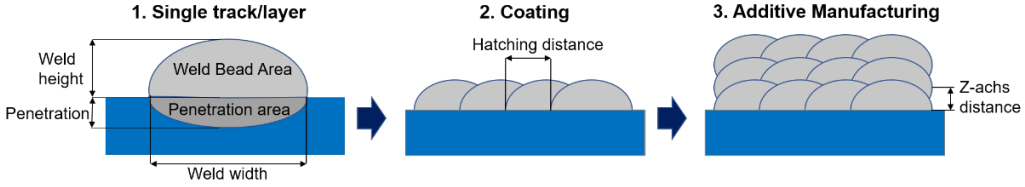

Figure 2. Optimization steps of the additive manufacturing.

A full factorial 2^3 (three factors with the two levels) central composite design with an axial point was used to produce the test matrix to optimize a single weld bead (Table 1). This design was augmented with an axial point (α), which is a strategically placed value at a specific distance ratio

from the center of the design space, to enhance the test matrix. The axial point 1.215 was used in order not to exceed the boundary conditions required for weld bead formation. Response surface regression method as a statistical method with Minitab Statistical software was utilized to analyze and optimize the process conditions. Regression learner with neural networks (NN) and Gaussian process regression (GPR) approaches as a supervised machine learning method were used with MATLAB R2021b software. As a nonparametric Bayesian method, GPR was developed using Gaussian probability distribution and it is particularly suitable for small amounts of data sets. The neural network used was a bi-layered fitting neural network. It can generalize an input-output relationship after training the data [7]. For machine learning, the training dataset in the central composite design was used as in the response surface method. The number of samples fabricated and results used for the training of the predictive algorithms consisted of 18 trials. The machine learning system was tested with an external dataset, which consist of 12 trials. Due to the small amount of data sets the 4-fold cross validation was chosen. The criteria for determining the discontinuities of the optimum welding parameters for a single weld bead were considered by DIN EN ISO 13919-1.

Table 1. Design of experiment of the single weld bead.

Parameters	Low Level	Central Point	High Level
Laser Power, W	500	1000	1500
Speed, mm/min	500	1000	1500
Powder Flow, g/min	5	10	15

Axial point (α):1.215

The evaluated dimensions of the weld are shown in Figure 2. The aspect ratio is in the acceptable range between 3 - 5. The accuracy of the weld was measured with a Lunovu linear laser scanner and a Keyence VK-X1000 laser scanner. The optimal dilution is between 2% - 15%, preferably between 5%-10% [8].

The weld width is a key parameter to transfer the technology to the coating application due to hatch distance. Therefore, the one factor at a time (OFAT) method with three levels was used for the coating optimization. After the coating, the two types of scanning strategy (Figure 3) were carried out and then the z-axis distance was determined.

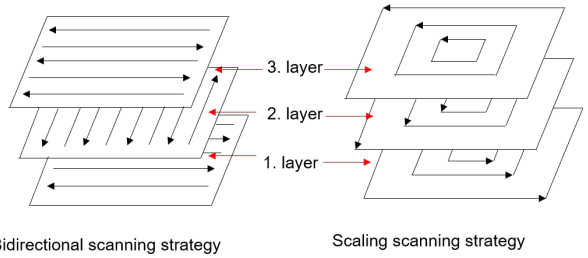

Figure 3. Bidirectional and scaling scanning strategy for additive manufacturing.

In Figure 4, the diagram shows the workflow in additive manufacturing, starting with the creation of a 3D model using CAD. This model is subsequently used to build manufacturing instructions through CAM with the optimized single weld parameters. The component was manufactured in the additive manufacturing stage with optimization of the hatch distance and z-axis distance as well as scanning strategy, followed by digitalization and evaluation of the component surface using a 3D scanning and metrology tool (ATOS-GOM Metronome System) to compare the manufactured product with the original CAD design for accuracy. After digitalization and evaluation of the AM part, the CAM values were optimized to achieve high accuracy near-net shape part. The final stage was the production of the final product and an iterative optimization process was applied to refine and improve the result.

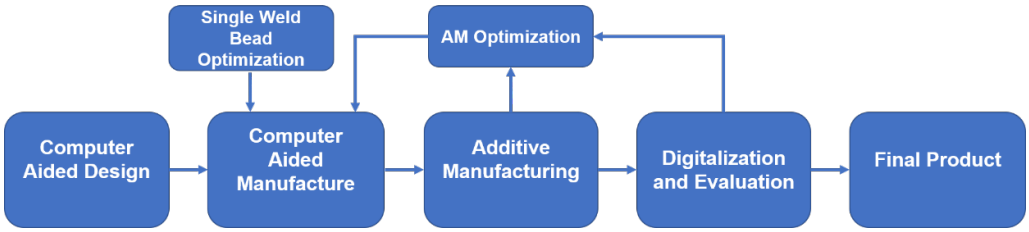

Figure 4. Rapid prototyping workflow of the additive manufacturing component in this study.

Analysis of as-deposited specimen

The samples were cut with a cutting machine. The cut sample was ground on silicon carbide grinding papers with grit sizes from 120 to 2500, polished using three steps of diamond suspension (6 µm, 3 µm, and 1 µm), and oxide polished (0.05 µm silica solution, Struers OP-S Suspension). The Digital Microscope (DM) VHX-7000 (Keyence Deutschland GmbH) was used to investigate the presence, weld bead geometry, and dilution of the cross section of it.

Results and discussion

Optimization of the Single Weld Bead

Weld width, weld height, aspect ratio, and dilution were optimized concerning laser power, travel speed, and powder flow rate. Response surface and machine learning methods were used for each output to optimize weld bead geometry.

Response Surface Method

The regression analysis carried out for the parameters of the L-DED process shows a robust model with a coefficient of determination (Table 2). A high value of R-squared and low value of standard error (S), mean squared error (MSE), and mean absolute error (MAE) indicate that the model can explain a significant proportion of the variability and high predictive capabilities. According to Minitab, R^2(adj) is the percentage of variation in the response that was explained by the model, adjusted for the number of predictors in the model relative to the number of observations. R^2(pred) was calculated using a formula equivalent to systematically removing each observation from the dataset, estimating the regression equation, and determining how accurately the model predicted the removed observation.

The equation of the weld width, weld height, aspect ratio, and dilution and their process window related to laser power, travel speed, and powder flow are shown in Equation (1) – Equation (4) and Figure 5, respectively. Equations exhibit a positive trended relationship with the laser power for the weld width, weld height, and dilution, and a negative trended relationship with aspect ratio. An increase in laser power leads to an increase in weld width, weld height, and unlikely, an increase in aspect ratio and dilution due to high heat input resulting in a higher melting rate.

Travel speed has a negative trend with weld width, and weld height and a positive trend with aspect ratio and dilution. High travel speed causes less heat input as well as powder feed on the substrate. Therefore, the weld with and height both decrease. The decreasing rate of the weld width is higher than to weld height, thus, the aspect ratio increases. However, dilution has a more complex relation in Figure 5. Due to this complex relation, Table 2 shows poor values of R^2, MSE, and MAE for dilution. On one hand, reducing the heat input per unit length causes decreasing the penetration area with reducing welding speed, on the other hand, less powder material per unit length causes decreasing of the weld bead area. The combination of geometrical parameters ensures that the dilution increases and then decreases.

In case increasing the powder feed rate, the weld height increases, however, the weld width decreases, slightly. This is because of a reduction in the unit heat required to melt large amount of powder which causes the low viscosity of melt pool and non-spread melt pool. Therefore, the

aspect ratio increases. Because of the high material transfer, the dilution decreases with the increase of the powder flow due to less heat transfer on the substrate.

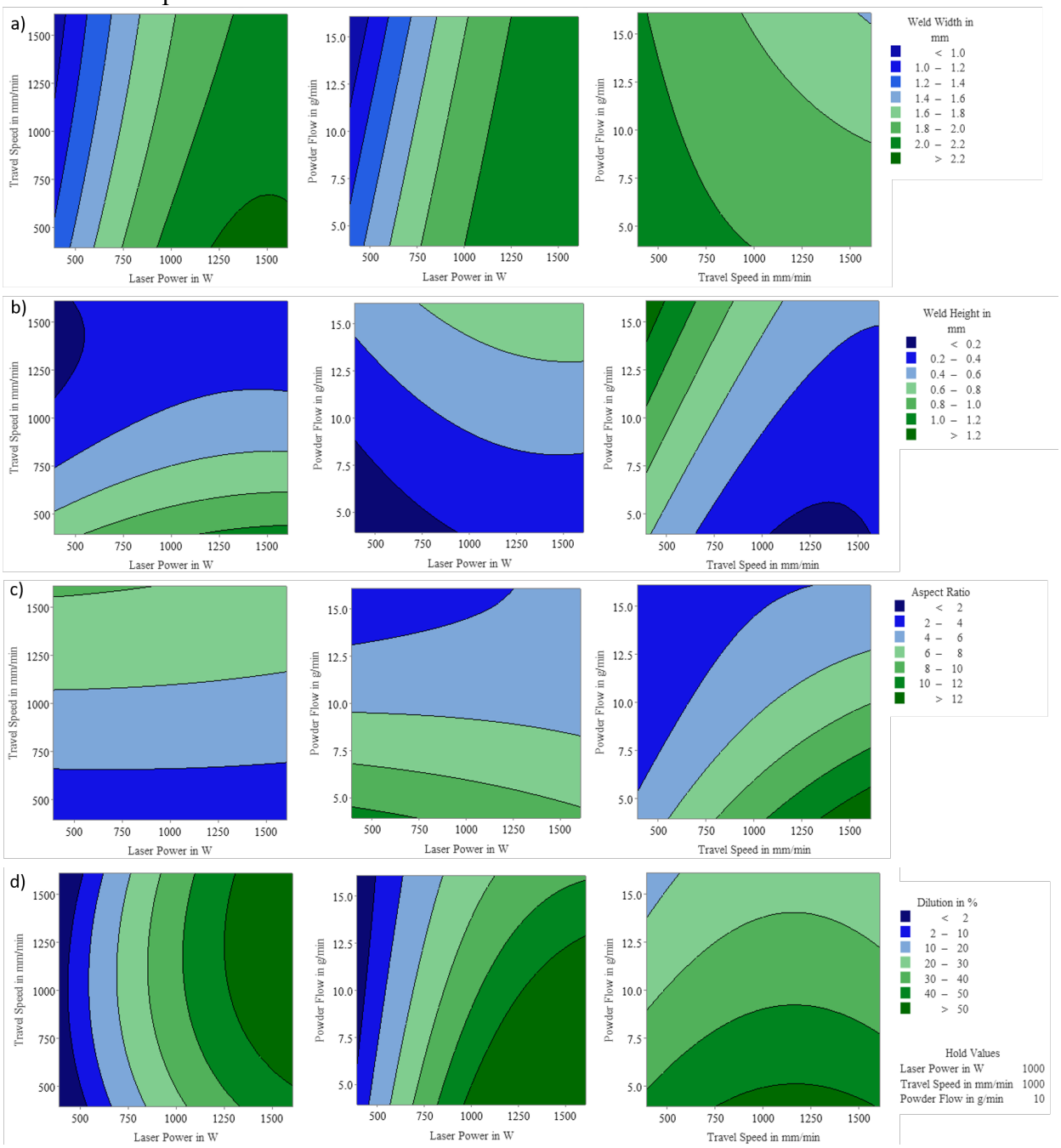

Figure 5 Process window of the laser power, travel speed, and powder flow rate concerning weld width (a), weld height (b), aspect ratio (c), and dilution (d) of the L-DED process.

Table 2. Model summary of response surface method.

Parameter	S	R²	R² (adj)	R² (pred)	MSE Test	MAE Test
Weld width	0.0483008	99.16%	98.41%	93.15%	0.01289	0.0877
Weld height	0.0330986	99.27%	98.62%	94.20%	0.03832	0.1824
Aspect ratio	0.659615	96.90%	94.10%	65.57%	0.80002	0.7761
Dilution	6.35228	95.81%	92.04%	68.66%	114.35455	8.9996

$$\begin{aligned}\text{Weld Width} = {} & 0.885 + 0.002101\ \text{Laser Power} - 0.000275\ \text{Travel Speed} \\ & - 0.0266\ \text{Powder Flow} - 0.000001\ \text{Laser Power*Laser Power} \\ & + 0.0000001\ \text{Travel Speed* Travel Speed} \\ & - 0.000297\ \text{Powder Flow*Powder Flow} + 0.0000001\ \text{Laser Power*Speed} \\ & + 0.000035\ \text{Laser Power*Powder} - 0.000021\ \text{Travel Speed*Powder Flow}\end{aligned} \quad (1)$$

$$\begin{aligned}\text{Weld Height} = {} & 0.380 + 0.000667\ \text{Laser Power} - 0.001204\ \text{Travel Speed} \\ & + 0.0608\ \text{Powder Flow} - 0.000000\ \text{Laser Power*Laser Power} \\ & + 0.000001\ \text{Travel Speed*Travel Speed} \\ & + 0.000335\ \text{Powder Flow *Powder Flow} \\ & - 0.0000001\ \text{Laser Power*Travel Speed} \\ & + 0.000004\ \text{Laser Power *Powder Flow} \\ & - 0.000034\ \text{Travel Speed *Powder Flow}\end{aligned} \quad (2)$$

$$\begin{aligned}\text{Aspect Ratio} = {} & 3.90 - 0.00209\ \text{Laser Power} + 0.01197\ \text{Travel Speed} \\ & - 0.787\ \text{Powder Flow} - 0.0000001\ \text{Laser Power *Laser Power} \\ & - 0.000001\ \text{Travel Speed*Travel Speed} \\ & + 0.0288\ \text{Powder Flow *Powder Flow} \\ & - 0.0000001\ \text{Laser Power *Travel Speed} \\ & + 0.000250\ \text{Laser Power*Powder Flow} \\ & - 0.000519\ \text{Travel Speed *Powder Flow}\end{aligned} \quad (3)$$

$$\begin{aligned}\text{Dilution} = {} & -48.8 + 0.1232\ \text{Laser Power} + 0.0147\ \text{Travel Speed} \\ & + 0.21\ \text{Powder Flow} - 0.000028\ \text{Laser Power*Laser Power} \\ & - 0.000011\ \text{Travel Speed * Travel Speed} + 0.010\ \text{Powder* Powder Flow} \\ & + 0.000011\ \text{Laser Power* Travel Speed} - 0.002661\ \text{Laser Power*Powder Flow} \\ & + 0.000105\ \text{Travel Speed * Powder Flow}\end{aligned} \quad (4)$$

Machine Learning Optimization of Single Weld Bead

By training the model using the dataset, it was observed that the most effective models for prediction of the input parameters the weld width and the weld height on the training and test set were the models generated using the GPR method (Figure 6 and Figure 7).

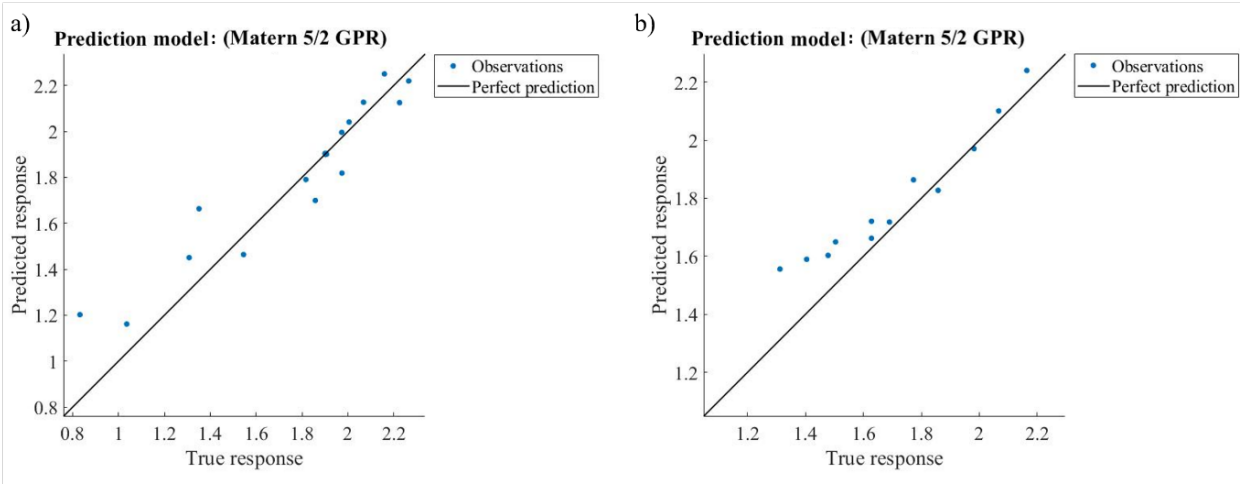

Figure 6. The training performance (a) and test (b) performance of the weld width prediction.

In Figure 6 and Figure 7, the majority of the observations for both the training and test datasets are near the line of perfect prediction, suggesting that the model has a high degree of accuracy in the prediction of the weld bead width based on the given input parameters - laser power, welding speed, and powder feed rate (Table 3). At lower true response values, the model tends to predict slightly higher weld width and lower weld height than observed, while at higher true response values the predictions of the model are consistent.

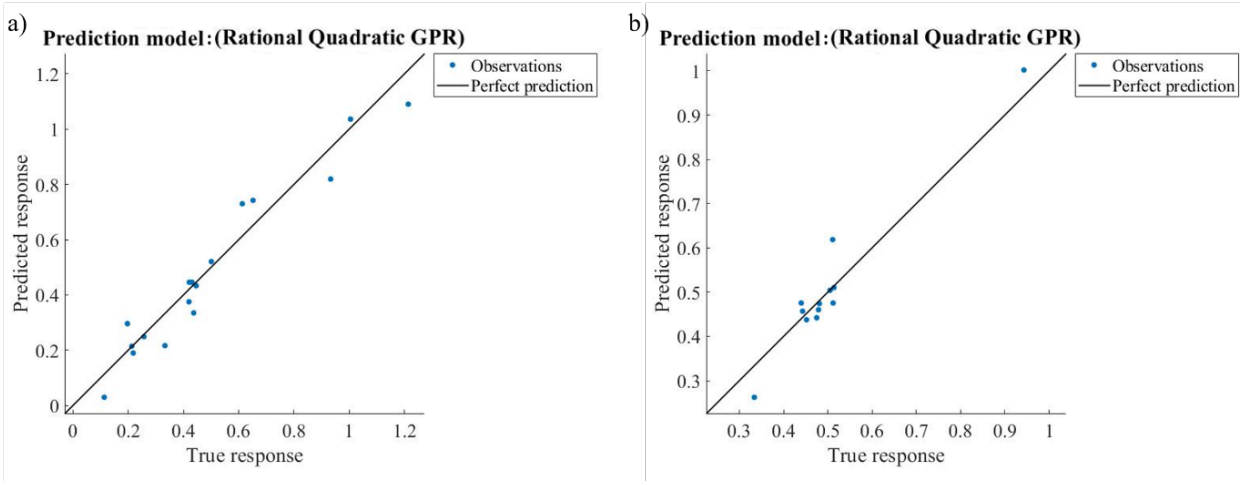

Figure 7. The training performance (a) and test (b) performance of the weld height prediction.

The response scatter plots highlight the robust ability of the bilayered neural network model to predict aspect ratio and dilution (Figure 8 and Figure 9).

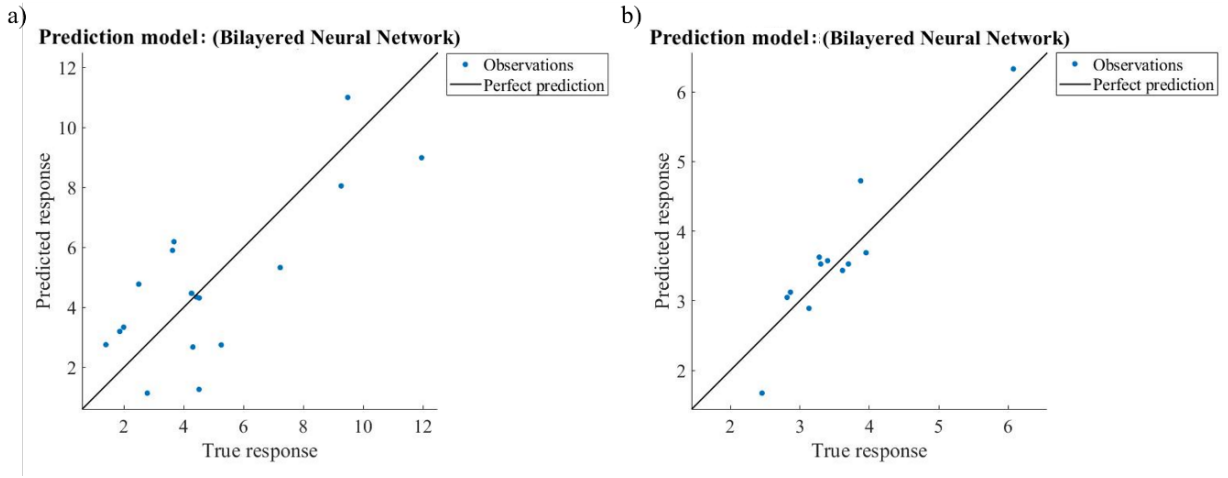

Figure 8. The training performance (a) and test (b) performance of the aspect ratio prediction.

At lower true response values which is critical for AM with L-DED, the model tends to predict consistent dilution than observed, while at higher true response values the predictions of the model are slightly higher.

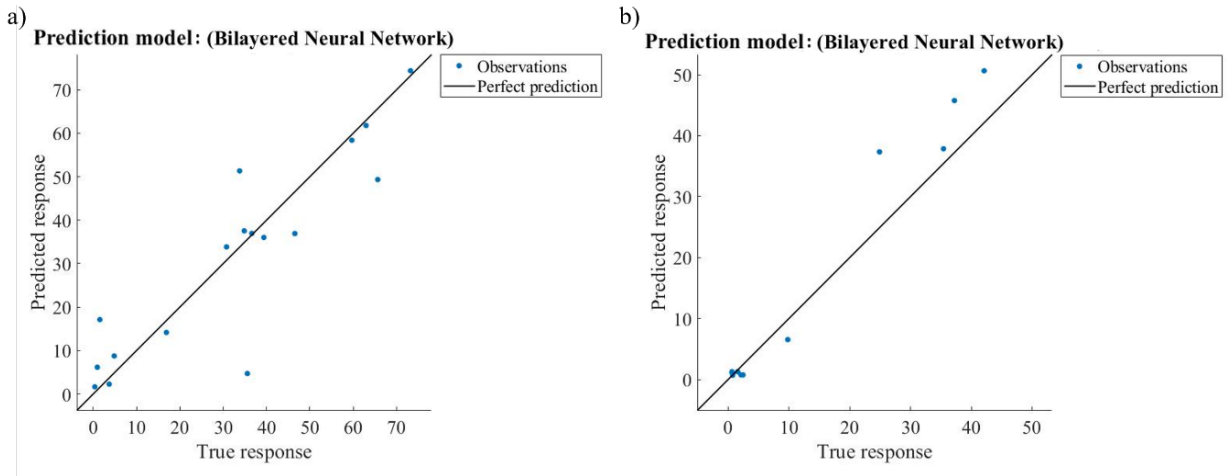

Figure 9. The training performance (a) and test (b) performance of the dilution.

Table 3. Training and test results of the machine learning models.

Parameter	RMSE Training/Test	R^2 Training/Test	MSE Training/Test	MAE Training/Test
Weld width	0.14015 / 0.11452	0.88 / 0.80	0.019642 / 0.11452	0.096801 / 0.091415
Weld height	0.073121 / 0.045294	0.94 / 0.89	0.00053467 / 0.0020515	0.058013 / 0.033399
Aspect ratio	1.8346/ 0.39856	0.72 / 0.79	3.3658 / 0.15885	1.5785 / 0.33145
Dilution	10.404 / 5.1832	0.80 / 0.89	108.24 / 26.865	6.5527 / 3.3351

Hybrid approach

In the hybrid approach, randomly augmented data from the RSM, constituting 25% of training data, was integrated with experimental data. The combined dataset was then utilized for the training of machine learning. To test the algorithm, the same test dataset as machine learning was used. The result of the training and test model of the hybrid approach is shown in Table 4.

Except for the weld width prediction, the hybrid model has a slightly lower performance in comparison to machine learning.

Table 4 Training and test results of the RSM-Machine learning hybrid approach.

Parameter	RMSE Training/Test	R^2 Training/Test	MSE Training/Test	MAE Training/Test
Weld width	0.09433/0.11472	0.94/0.80	0.008898/0.01316	0.059998/0.090264
Weld height	0.10487/0.062279	0.87/0.80	0.010997/0.074023	0.074023/0.047107
Aspect ratio	1.569/0.43455	0.66/0.75	2.4614/0.18883	0.75323/0.36265
Dilution	10.93/7.5793	0.81/0.77	119.47/57.446	6.7143/6.428

The parameters were optimized to achieve defect-free deposition with minimized dilution, causing minimized heat input. The chosen optimized input parameters by machine learning are for a lower response 650 W laser power, 500 mm/min travel speed, and 5 g/min powder flow which gives 1.628 mm weld width, 0.440 mm weld height, 3.70 aspect ratio and 2.1% dilution; for an upper response 750 W laser power, 500 mm/min travel speed and 5 g/min powder flow which gives 1.858 mm weld width, 0.514 mm weld height, 3.62 aspect ratio and 9.8% dilution.

The optimization was performed by machine learning. To minimize the process complexity, the optimum parameter range was determined by adjusting only laser power. Table 5 and Figure 10 show the optimized weld bead parameters and cross-section of the weld beads. As a lower response, a laser power with 650W, and an upper response a laser power with 750W were chosen. The travel speed of 500 mm/min and powder flow of 5g/min were remained constant. The powder efficiency of the 750W optimized parameters is 53%.

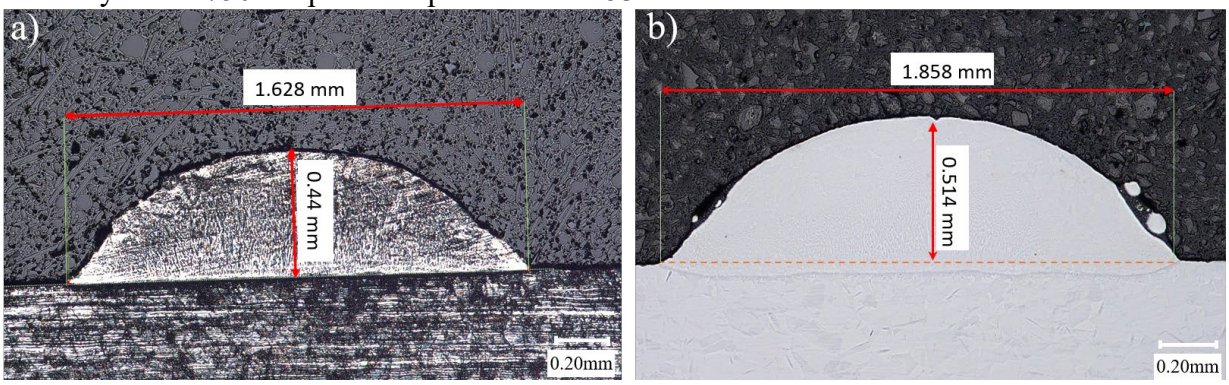

Figure 10. Microscope image of optimized weld beads with (a) a lower response (650W) and (b) an upper response (750W) based on Table 5.

Table 5. Optimized weld bead parameter with a lower response and upper response.

Laser Power, W	Speed, mm/min	Powder Flow, g/min	Width, mm	Height, mm	Aspect Ratio	Dilution, %
650	500	5	1.628	0.440	3.70	2.1
750	500	5	1.858	0.514	3.62	9.8

Determination of suitable Coating Parameters

The coating application was carried out with 5 stringer weld tracks and optimized by lower response parameters due to consider lack of fusion between the tracks. By optimization of the coating with three different hatch distances, it was observed that a narrow hatch distance with 40% of the weld width causes lack of fusion between tracks. The reason for this, if the focus position is not maintained, the steep flanks of the tracks can cause the laser beam to be shadowed during side-by-side welding with track overlap, which can result in bonding discontinues between adjacent tracks [9]. 50% and 60% hatch distances do not cause lack of fusion, however, the linearity of the surface of the cross-section between 1. track and 5. track is higher in 60% hatch distance than 50% (Figure 11). Therefore, the optimum hatch distance for coating is 60% of the weld width for coating

application. The average coating height of optimum hatch distance was measured as 0.74 mm which will be used for z axis optimization.

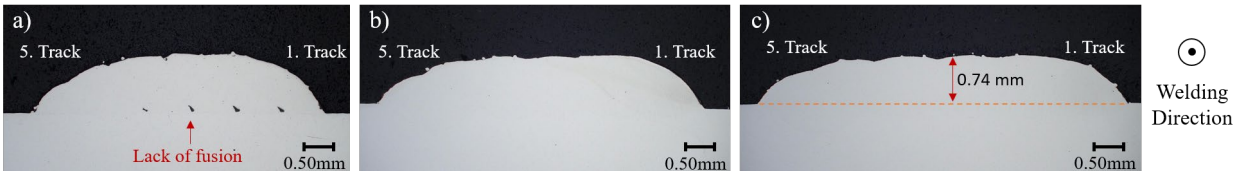

Figure 11. Cross-sections of the coating with hatch distance of (a) 40%, (b) 50% and (c) 60% of the weld width.

Optimization of Additive Manufacturing

The optimization of additive manufacturing samples was performed as a basic geometry in the form of a cylinder/cube. Figure 12 represents the cross-section of the basic shaped additive manufacturing samples. They were manufactured using optimized parameters that included a laser power of 650W. Each layer was built with a 0.7 mm z-axis offset distance employing a scaled and bidirectional scanning strategy (Figure 12a, Figure 12b). Instead of the upper part, the bottom part of both samples exhibits lack of fusion same as coating section (Figure 11a). The reason for not occurrence of lack of fusion in the upper layers is the increase in penetration as a result of heat accumulation. Increasing the layer height to 0.8 mm and using a bidirectional scanning strategy produced no bonding defects in the cube sample. (Figure 12c).

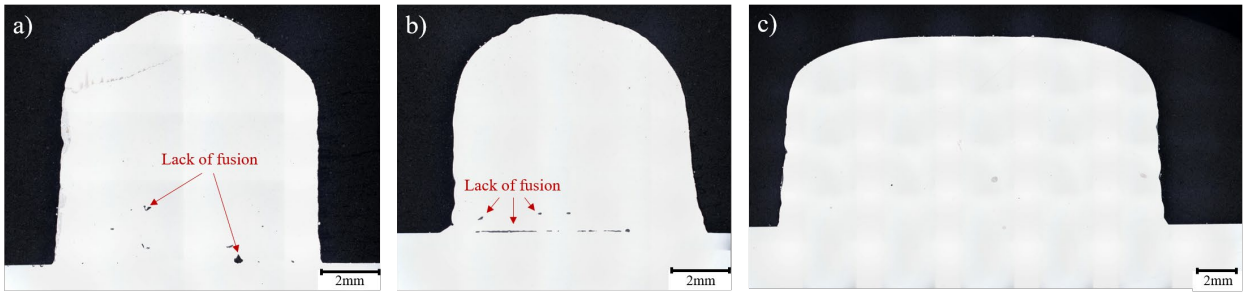

Figure 12. Cross-section of the basic shaped additive manufacturing samples. (a) 0.7 mm z-axis for each layer with scaled scanning strategy, (b) 0.7 mm z-axis for each layer with bidirectional scanning strategy, and (c) 0.8 mm z-axis for each layer with bidirectional scanning strategy.

Prototyping of the component

Figure 13 illustrates the additive manufacturing of the component. The prototyping process began with a digital model of the desired object, typically designed with CAD. Geometric adjustments of CAD can be performed at this stage due to avoid some design problems such as overhang. As a next step, the CAD model was processed using CAM software to plan the toolpath and simulate it with the optimized parameters. The blue lines represent the path planning with layers of deposited material. The actual production was carried out using the L-DED process. The laser was used to create a melt pool on the substrate material where powder material is deposited. The laser traveled along the planned path, transforming the powder into a final solid structure layer by layer.

Between the lower (650W) and upper (750W) response parameters with an average 0.8 mm Z axis offset distance were used. The laser power is gradually reduced at the upper layers to prevent overheating.

The final product was machined using the CNC (Computer Numerical Control) milling process, a subtractive manufacturing process. The oversized material was removed from the additive manufactured near net-shaped sample using a cutting tool to achieve the desired shape and surface. The final product does not show any defects on the surface caused by porosity and lack of fusion.

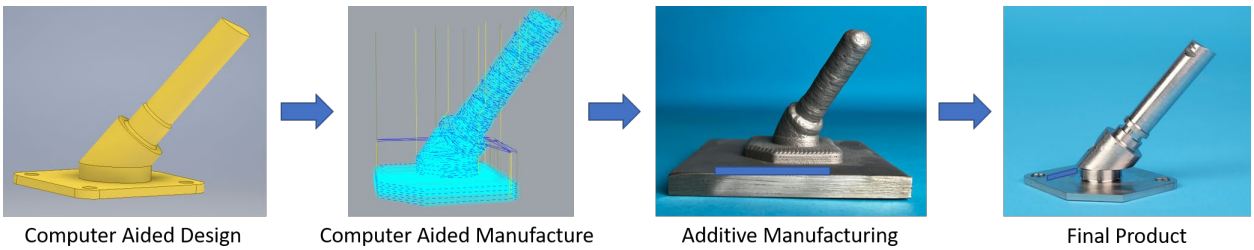

Figure 13. Additive manufacturing of the component.

Figure 14 demonstrates the digitalization and surface evaluation of the component. The color map indicates surface deviation from the targeted CAD part. The scale on the right displays the range of these deviations in millimeters. The red and blue areas identify the oversized and undersized dimensions, respectively. The green area identifies where the component dimensions are close to the design dimensions. The blue area should not appear. The minimum, maximum, and average surface deviation of the additive manufacturing and CAD parts are +0.1 mm, +3.28 mm, and +1.23 mm, respectively. Material consumption decreases for the final production as the average deviation decreases to zero. The final product was achieved by applying the milling process.

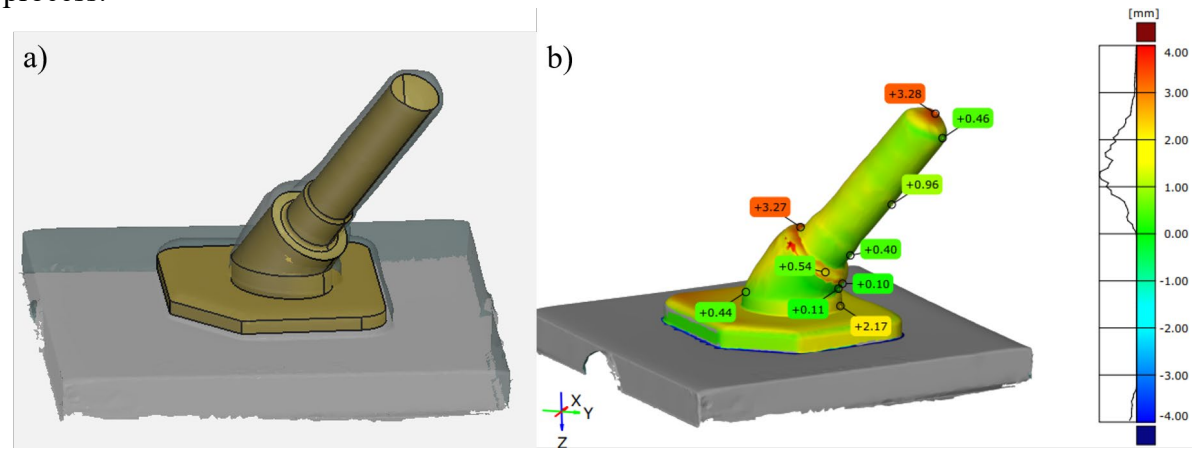

Figure 14. Digitalization and surface evaluation of the component: a) Alignment of the scanned component with CAD, b) surface deviation of the scanned component.

Conclusion

This study demonstrates an L-DED approach from initial to final steps for rapid prototyping in additive manufacturing. The optimization part of the methodology has significantly improved the precision and prediction of welding parameters such as laser power, welding speed and powder flow with respect to critical output parameters such as weld bead width, height and dilution. RSM, machine learning and hybrid approaches were utilized and compared. The study focuses on determining optimal L-DED parameters with a minimum number of planned trials involving test data. The regression learner-based ML algorithm provides a robust ability with high R-squared and low MSE values to predict these output metrics with considerable accuracy compared to statistical approach and hybrid approach for test data. The prediction of dilution is less accurate than that of other factors, due to the highly complex behavior of dilution. Based on the optimized parameters, the appropriate coating with hatch distance of 60% of the weld bead was applied and subsequently additive manufacturing with a z-axis distance of 0.8 mm was performed. The evaluation of the near net-shaped part was carried out by digitization and the final product of the aerospace part was prototyped. This approach is a step towards developing rapid prototyping additive manufacturing for future digital twin applications by increasing the precision and reducing the complexity of the L-DED process for aerospace industry.

Acknowledgements
The authors thank Avantika Jhanji for assisting with the GOM measurement.

Funding
This work was supported by the European Union and the European Regional Development Fund and was carried out in the framework of the project GABRIEL - Erforschung GAnzheitlicher, HyBrid-ElektRIscher AntriebskomponEnten für die Luftfahrt (ProFIT Brandenburg, Application number: 80257607).

References

[1] G. Piscopo and L. Iuliano, "Current research and industrial application of laser powder directed energy deposition," *Int J Adv Manuf Technol*, vol. 119, 11-12, pp. 6893–6917, 2022. https://doi.org/10.1007/s00170-021-08596-w

[2] I. Z. Era, M. A. Farahani, T. Wuest, and Z. Liu, "Machine learning in Directed Energy Deposition (DED) additive manufacturing: A state-of-the-art review," *Manufacturing Letters*, vol. 35, pp. 689–700, 2023. https://doi.org/10.1016/j.mfglet.2023.08.079

[3] A. Abdulraheem, R. Abdullah Arshah, and H. Qin, "Evaluating the Effect of Dataset Size on Predictive Model Using Supervised Learning Technique," *International Journal of Software Engineering & Computer Sciences (IJSECS)*, vol. 1, pp. 75–84, 2015. https://doi.org/10.15282/ijsecs.1.2015.6.0006.

[4] Y. Zhu, Z. Yuan, M. M. Khonsari, S. Zhao, and H. Yang, "Small-Dataset Machine Learning for Wear Prediction of Laser Powder Bed Fusion Fabricated Steel," *Journal of Tribology*, vol. 145, no. 9, p. 91101, 2023. https://doi.org/10.1115/1.4062368

[5] X. Zhu, F. Jiang, C. Guo, de Xu, Z. Wang, and G. Jiang, "Surface morphology inspection for directed energy deposition using small dataset with transfer learning," *Journal of Manufacturing Processes*, vol. 93, pp. 101–115, 2023. https://doi.org/10.1016/j.jmapro.2023.03.016

[6] J. Xiong, G. Zhang, J. Hu, and L. Wu, "Bead geometry prediction for robotic GMAW-based rapid manufacturing through a neural network and a second-order regression analysis," *Journal of Intelligent Manufacturing*, vol. 25, no. 1, pp. 157–163, 2014. https://doi.org/10.1007/s10845-012-0682-1

[7] PERNA Alessia Serena, CARRINO Luigi, CITARELLA Alessia Auriemma, De MARCO Fabiola, Di BIASI Luigi, TORTORA Genoveffa, VISCUSI Antonio, A machine learning approach for adhesion forecasting of cold-sprayed coatings on polymer-based substrates, Materials Research Proceedings, Vol. 28, pp 57-64, 2023. https://doi.org/10.21741/9781644902479-7

[8] Raphaela Rauter, "Laserauftragschweißen von Wolframkarbidschichten in Nickelbasismatrizen zur Herstellung verschleißfester Beschichtungen von Warmformwerkzeugen," Technischen Universität Graz, 2016.

[9] J. Witzel, "Qualifizierung des Laserstrahl-Auftragschweißens zur generativen Fertigung von Luftfahrtkomponenten," Von der Fakultät für Maschinenwesen der Rheinisch-Westfälischen Technischen Hochschule Aachen zur Erlangung des akademischen Grades eines Doktors der Ingenieurwissenschaften genehmigte Dissertation, Dec. 2014.